ELSEVIER

Colloids and Surfaces
A: Physicochemical and Engineering Aspects 97 (1995) 65–82

COLLOIDS AND SURFACES A

Dynamic surface tensions of surfactant mixtures at the water–air interface

V. B. Fainerman [a], R. Miller [b,*]

[a] *Institute of Technical Ecology, Blvd. Shevchenko 25, 340017 Donetsk, Ukraine*
[b] *MPI für Kolloid- und Grenzflächenforschung, Rudower Chaussee 5, D-12489 Berlin-Adlershof, Germany*

Received 20 July 1994; accepted 27 November 1994

Abstract

Studies of dynamic surface tensions $\gamma(t)$ using an automated maximum bubble pressure method in the time interval from 1 ms to 30 s are performed with mixtures of non-ionic surfactants (Triton X-45, X-100, X-114, X-165, X-305 and X-405) and sodium alkyl sulphates (decyl, dodecyl, tetradecyl and hexadecyl). In the range of longer times t the dependencies $\gamma(1/\sqrt{t})$ of the single components show linear behaviour, giving evidence for a diffusion controlled adsorption in the absence of disturbing amounts of surface active impurities. Similar results are obtained on the addition of a second component with a sufficiently high surface activity. The adsorbed amount calculated from the $(\gamma(1/\sqrt{t})$ dependences using a modified Hansen–Joos approximate relation agree well with those obtained from equilibrium surface tension data.

The experimental $\gamma(1/\sqrt{t})$ curves of some surfactant mixtures show small jumps in the range over which displacement of the lower component by the stronger surface active molecules is introduced. These surface tension jumps are used to calculate the rate constants of desorption of sodium decyl and dodecyl sulphate. The obtained value of $k_{ad} = 50\ s^{-1}$ is in good agreement with earlier published data for these surfactants.

Keywords: Adsorption kinetics; Dynamic surface tension; Maximum bubble pressure; Nonionics; Surfactant mixtures

1. Introduction

Although the adsorption kinetics of surfactant mixtures is of great practical importance, up until now this area has not been widely studied, from the experimental or from the theoretical point of view [1]. A general theory and some approximate solutions of the adsorption kinetics process are given in Refs. [2]–[4]. Asymptotic solutions of the adsorption kinetics theory of surfactant mixtures have recently been derived [5,6]. A few experimental results have been published so far, for example on mixtures of sodium salts of fatty acids [2], mixtures of sodium alkyl sulphates [4,6] and mixtures of alkyl sulphates with *n*-alkanols [4,5]. These results illustrate the complex character of the adsorption process of mixed surfactant solutions.

Recently, some unusual experimental results were published for commercial samples of sodium dodecyl sulphate (SDS). Such samples contain different surface active contaminants, most of all the homologous alcohols, the surface activities of which are more than two orders of magnitude higher than that of the main surfactant SDS [7]. It was also shown by analytical methods

* Corresponding author.

SSDI 0927-7757(94)03069-3

that the preparation of reliable SDS samples, although difficult, is successful [8], and even aqueous solutions can be kept over a long period of time without loss of the high degree of purity [9].

The dynamic surface tension of a commercial sample measured with a continuously growing drop technique exhibits a pronounced maximum of some tenths of a mN m^{-1} over the time interval in which the dodecanol starts to adsorb [10]. In our opinion, the intermediate maximum may be connected to a slower desorption of the SDS molecules after the dodecanol starts to adsorb. Another experiment with SDS was performed with a capillary wave technique and peculiarities were observed which so far are not fully understood [11]. Anyhow, the dynamic surface tension $\gamma(\log t)$ shows two inflexion points, which is a typical feature of the adsorption of a mixture of two surfactants with significantly different surface activities.

The present paper presents a detailed study of the adsorption kinetics of surfactant mixtures by means of dynamic surface tension measurements. The results are analysed on the basis of existing theory and discussed in terms of possible adsorption or desorption barriers. In the case of existing barriers, the kinetics mechanism can be obtained from the shape of the experimental dependence of the surface tension on time. Such qualitative interpretation is advantageous in many cases, taking into account the very complicated mathematical analysis of dynamic surface tension data, for example by diffusion controlled model [12].

2. Theory

The equilibrium state of adsorption of a mixture of two surfactants can be described under the assumption of ideal behaviour in the bulk and mutual interaction at the surface by the following set of equations, which corresponds to a Frumkin–Damaskin isotherm [13]:

$$b_i c_{i,0} = \frac{\Gamma_{i0}/\Gamma_{i\infty}}{n_i[1-(\Gamma_{10}/\Gamma_{1\infty})-(\Gamma_{20}/\Gamma_{2\infty})]^{n_i}} \tag{1}$$

$$\gamma_\infty = \gamma_0 + RT\Gamma_\infty\left[\ln\left(1-\frac{\Gamma_{10}}{\Gamma_{1\infty}}-\frac{\Gamma_{20}}{\Gamma_{2\infty}}\right) + \frac{n_1-1}{n_1}\frac{\Gamma_{10}}{\Gamma_{1\infty}} + \frac{n_2-1}{n_2}\frac{\Gamma_{20}}{\Gamma_{2\infty}}\right] \tag{2}$$

Γ_∞, $\Gamma_{1\infty}$ and $\Gamma_{2\infty}$ are the maximum surface coverage of the solvent molecules and the individual components, respectively, $n_i = \Gamma_{i\infty}/\Gamma_\infty$, and Γ_{10} and Γ_{20} are the equilibrium surface concentrations of the individual components at the respective bulk concentrations c_{10} and c_{20}. γ_0 and γ_∞ are the surface tension of the surfactant free system and the equilibrium surface tension of the surfactant solution, respectively. R and T are the gas law constant and absolute temperature, respectively. The application of a Frumkin–Damaskin isotherm describes very well the equilibrium adsorption behaviour of surfactant mixtures [14], but is not suitable for adsorption kinetics models owing to its complex structure. Hence a simpler set of equations will be used below.

If we assume $\Gamma_\infty \approx \Gamma_{1\infty} \approx \Gamma_{2\infty}$, Eqs. (1) and (2) can be simplified to

$$\Gamma_{i0} = \Gamma_{i\infty}\frac{b_i c_{i0}}{1+b_1 c_{10}+b_2 c_{20}} \tag{3}$$

$$\gamma_\infty = \gamma_0 + RT\Gamma_\infty \ln[1-(\Gamma_{10}/\Gamma_{1\infty})-(\Gamma_{20}/\Gamma_{2\infty})] \tag{4}$$

The time dependence of the surface concentration of each component is given by an integral equation of the Ward and Tordai type [15,16]:

$$\Gamma_i(t) = 2\sqrt{\frac{D_i}{\pi}}\left[c_{i0}\sqrt{t} + \int_0^t c_i(0, t-\tau)\,\mathrm{d}\sqrt{\tau}\right] \tag{5}$$

where D_i is the diffusion coefficient, $c_i(0, t)$ is the subsurface concentration of component i, and t is time. The two integral equations (5) are linked to each other via Eqs. (1) and (2).

In the present paper we are interested in the time interval over which the adsorption of one of the two components runs through a maximum. A sufficient condition for the existence of a maximum in the $\Gamma_1(t)$ curve is

$$c_{10} \gg c_{20}, \qquad b_2 c_{20} \approx b_1 c_{20} > 1 \tag{6}$$

After passing the maximum we can assume that the subsurface concentration $c_1(0, t)$ is constant and equal to the bulk concentration c_{10}, and a diffusion equilibrium of component 1 results.

The adsorption of both components beyond the maximum in the $\Gamma_1(t)$ curve, and using the simplification $\Gamma_{\infty} = \Gamma_{1\infty} = \Gamma_{2\infty}$, is now given by the two following relations:

$$\Gamma_1(t) = \Gamma_{\infty} \frac{b_1 c_{10}}{1 + b_1 c_{10} + b_2 c_2(0, t)} \tag{7}$$

$$\Gamma_2(t) = \Gamma_{\infty} \frac{b_2 c_2(0, t)}{1 + b_1 c_{10} + b_2 c_2(0, t)} \tag{8}$$

At small deviations from equilibrium, the following relations can be derived from Eqs. (7) and (8):

$$\left(\frac{\partial \Gamma_1}{\partial c_2}\right)_{c_1} = -\frac{\Gamma_1 \Gamma_2}{\Gamma_{\infty} c_2} \tag{9}$$

$$\left(\frac{\partial \Gamma_2}{\partial c_2}\right)_{c_1} = \left(1 - \frac{\Gamma_2}{\Gamma_{\infty}}\right)\frac{\Gamma_2}{c_2} \tag{10}$$

Combining Eqs. (9) and (10), we obtain

$$\left(\frac{\partial \Gamma_1}{\partial c_2}\right)_{c_1} \Big/ \left(\frac{\partial \Gamma_2}{\partial c_2}\right)_{c_1} = \frac{\Gamma_1}{\Gamma_{\infty} - \Gamma_2} \tag{11}$$

The time dependence of the surface concentrations calculated on the basis of Eq. (5) (see, for example, Ref. [17]), agrees well with the data from Eq. (11) at times $t > t_{\max \Gamma_1}$, where $t_{\max \Gamma_1}$ corresponds to the time at which Γ_1 passes the maximum.

At long adsorption times an asymptotic solution of Eq. (5) exists [18]:

$$c_{i0} - c_i(0, t) = \Gamma_i \sqrt{\frac{\pi}{4 D_i t}} \tag{12}$$

which together with the Gibbs equation

$$-\mathrm{d}\gamma = RT\Gamma_1 \,\mathrm{d} \ln c_1 + RT\Gamma_2 \,\mathrm{d} \ln c_2 \tag{13}$$

and considering $\mathrm{d} \ln c_1 = 0$ finally leads to

$$\Delta\gamma = \gamma(t) - \gamma_{\infty} = \frac{RT\Gamma_2^2}{c_{20}} \sqrt{\frac{\pi}{4 D_2 t}} \tag{14}$$

where $\gamma(t)$ is the dynamic surface tension. This equation is a generalisation of the known relation of Hansen–Joos [18] for the case $c_{10} \gg c_{20}$.

It can be shown that Eq. (14) can also be derived from the Frumkin isotherm in the following form:

$$\gamma(t) = \gamma_0 + RT\Gamma_{\infty} \ln(1 - (\Gamma_1/\Gamma_{1\infty}) - (\Gamma_2/\Gamma_{2\infty})) \tag{15}$$

At small deviations from equilibrium we get

$$\mathrm{d}\gamma = -\frac{RT\Gamma_{\infty}(\mathrm{d}\Gamma_1/\Gamma_{1\infty} + \mathrm{d}\Gamma_2/\Gamma_{2\infty})}{1 - (\Gamma_1/\Gamma_{1\infty}) - (\Gamma_2/\Gamma_{2\infty})} \tag{16}$$

Using Eqs. (9), (10) and (12), the relation (16) can easily be transformed into Eq. (14). For large times t, the adsorption $\Gamma_2(t)$ approaches the equilibrium value Γ_{20}, and can be approximated with the help of Eqs. (8) and (12) to

$$\Gamma_2 = \Gamma_{20}\left[1 + \frac{\Gamma_{20}}{c_{20}}\left(1 - \frac{\Gamma_{20}}{\Gamma_{\infty}}\right)\sqrt{\frac{\pi}{4Dt}}\right]^{-1} \tag{17}$$

Eq. (14) can also be applied to the adsorption of surfactant mixtures at interfaces with time dependent area, e.g. for experimental methods such as the drop volume method or the maximum bubble pressure method. The relative surface area dilation Θ is given by [19,20]

$$\Theta = \frac{\mathrm{d} \ln A}{\mathrm{d}t} = \xi t^{-1} \tag{18}$$

where A is the area and ξ is a constant which depends on the experimental conditions. A relation for the effective adsorption time t_{eff} in the case of the maximum bubble pressure, only taking into account bubble growth up to its hemispherical size, is given in Refs. [20] and [21]:

$$t_{\mathrm{eff}} = \frac{t}{2\xi + 1} \tag{19}$$

Let us now consider the case of the non-diffusion controlled adsorption of component 1 in the mixture which is of interest for the systems studied in the present paper, namely systems consisting of a less surface active component 1 and a higher surface active component 2 [6]. The non-diffusional adsorption of low surface active surfactants at sufficiently high bulk concentration has already been discussed in Refs. [12] and [22]. It was recently shown [6] that complex non-stationary problems of adsorption kinetics can be solved

successfully by making use of much simpler stationary and quasi-stationary problems. In the case of a non-diffusional adsorption mechanism of component 1, the corresponding rate equation for a non-stationary surface with change in relative area Θ is

$$\Gamma_1\Theta = k_{ad}c_1(0,t)\left(1-\frac{\Gamma_1}{\Gamma_\infty}-\frac{\Gamma_2}{\Gamma_\infty}\right)-k_{des}\Gamma_1 \qquad (20)$$

where k_{ad} and k_{des} are the rate constants of adsorption and desorption, respectively. At times $t > t_{max\Gamma_1}$, we can assume $c_1(0,t) = c_{10}$, so that any change in Γ_1 is caused by the change in $\Gamma_2(t)$. From Eq. (20) at small deviations from equilibrium we obtain

$$\frac{d\Gamma_1}{d\Gamma_2} = -\left(\frac{\Gamma_\infty\Theta}{k_{ad}c_{10}}+\frac{b_1c_{10}+1}{b_1c_{10}}\right)^{-1} \qquad (21)$$

If we now make use of Eqs. (10), (12) and (16), assuming a diffusion controlled adsorption of component 2, we obtain after some rearrangement

$$\Delta\gamma = \gamma(t)-\gamma_\infty = \frac{RT\Gamma_2^2}{c_{20}}\sqrt{\frac{\pi}{4D_2t}}\left(1+\frac{K_1b_1c_{10}}{1+K_1+1/b_1c_{10}}\right) \qquad (22)$$

where $K_1 = \Gamma_\infty\Theta/k_{des}c_{10}$. The value of $dc_2(0,t)$ in Eq. (10) was derived from Eq. (12). The same result can be obtained from a relation derived by Van Voorst Vader et al. [23] for a time-dependent surface area:

$$c_{i0}-c_i(0,t) = \Gamma_i\sqrt{\frac{\pi\Theta}{2D_i}} \qquad (23)$$

In the case of the bubble pressure technique, the change in relative area is given by $\Theta = 0.5t^{-1}$ [6,24].

If $K_1 \to 0$, ($k_{des} \to \infty$), Eq. (22) transforms into Eq. (14) derived for the diffusion controlled adsorption of surfactant mixtures. Under the conditions $b_1c_{10} \gg 1$ and $1 \gg K_1$, the following approximate relation can be obtained:

$$\Delta\gamma = \frac{RT\Gamma_2^2}{c_{20}}\sqrt{\frac{\pi}{4D_2t}}(1+K_1b_1c_{10}) \qquad (24)$$

Thus, the change in surface tension with time at $t > t_{max\Gamma_1}$ can be interpreted by the sum

$$\Delta\gamma = \Delta\gamma_d + \Delta\gamma_b \qquad (25)$$

where $\Delta\gamma_d$ is the contribution from diffusional transport and $\Delta\gamma_b$ refers to a barrier controlled contribution. From Eqs. (18) and (22) the value of $\Delta\gamma_b$ can be estimated:

$$\Delta\gamma_b = \frac{RT\Gamma_2^2}{c_{20}}\sqrt{\frac{\pi}{4D_2t}}(\xi/k_{des}t) \qquad (26)$$

There are several papers dealing with the interpretation of the rate constants of adsorption k_{ad} and desorption k_{des} on the basis of molecular kinetics theories [25,26] or the theory of transfer states [27]. In general, one can express these rate constants as

$$k_{des} = \bar{k}_{des}\exp(E_{ad}/RT) \qquad (27)$$

and

$$k_{ad} = \bar{k}_{ad}\exp(E_{des}/RT) = \bar{k}_{ad}\exp\left(\frac{E_{ad}+E}{RT}\right) \qquad (28)$$

where E, E_{ad} and E_{des} are the energy of adsorption, activation energy of adsorption and activation energy of desorption, respectively. The rate constants $\bar{k}_{ad}$ and $\bar{k}_{des}$ correspond to the absence of any activation energy of adsorption and desorption, respectively. The physical meaning of the adsorption rate constant $\bar{k}_{ad}$ is connected to the rate of molecular movements w in the interfacial layer of thickness δ, given by $\bar{k}_{ad} = w = D/\delta$ [28]. The rate constant of desorption $\bar{k}_{des}$ is equivalent to the time τ that an adsorbed molecule remains in the adsorption layer. For $E_{des} = 0$ this value is given by $\bar{k}_{des} = \tau^{-1} = w/\delta$, so that we finally obtain

$$\bar{k}_{des} = D/\delta^2 \qquad (29)$$

The value of the adsorption energy can be obtained from the change in the free energy of adsorption, given by

$$\Delta F = -RT\ln(a_s/a_b) = -RT\ln(\Gamma_0/\delta c_0) \qquad (30)$$

where a_s and a_b are the activities of the surfactant in the surface and bulk phase, respectively. For a diluted adsorption layer, $\Gamma_0 = \Gamma_\infty bc_0$, we can write

$$E = -\Delta F = RT\ln(b\Gamma_\infty/\delta) \qquad (31)$$

From Eqs. (27)–(31) the following expression for the physical explanation of k_{des} and the interrelation between the two rate constants is obtained:

$$k_{des} = \frac{D}{\delta b \Gamma_\infty} \exp(-E_{ad}/RT) = k_{ad}/b\Gamma_\infty \quad (32)$$

The theory of adsorption barriers is not developed quantitatively, so that the activation energy E_{ad} of any surfactant can be calculated. Only the ratio of the two rate constants can be deduced from the corresponding equilibrium state of the rate equation (20), $\Gamma_\infty b = k_{ad}/k_{des}$. Recently, based on the assumption of an entropic nature of the adsorption barrier at the water–air interface, a proportionality between b and k_{ad} was discussed [12] and demonstrated experimentally for surfactants of low molecular weight [29]. If we assume $k_{ad} \approx b$, then k_{des} must be constant. This result was confirmed for a large number of surfactants at small adsorption times in Refs. [22] and [30], and an average value of $k_{des} \approx 80\ s^{-1}$ was found.

The order of magnitude of $\Delta\gamma_b$ can be estimated according to Eqs. (17) and (26) using the following values of the required parameters: $k_{des} \approx 80\ s^{-1}$, $\xi = 0.5$, $\Gamma_2 = 2 \times 10^{-10}$ mol cm^{-2}, $c_{20} = 1 \times 10^{-7}$ mol cm^{-3}, $D_2 = 3 \times 10^{-6}$ cm^2 s^{-1}. In the range of small adsorption times $0.001\ s < t < 0.01$, we obtain $\Delta\gamma_b = 0.2$–0.5 mN m^{-1}.

There is a useful approximation of Eqs. (17) and (26) for the case

$$\frac{\Gamma_{20}}{c_{20}}\sqrt{\frac{\pi}{4Dt}} \gg 1,$$

i.e. at small time t and bulk concentration c_{20}. Eq. (17) then simplifies to

$$\Gamma_2(t) = 2c_{20}\sqrt{\frac{D_2 t}{\pi}} \quad (33)$$

and Eq. (26) takes the form

$$\Delta\gamma_b = 2RTc_{20}\sqrt{\frac{D_2}{\pi t}}\frac{\xi}{k_{des}} \quad (34)$$

This equation yields identical results to those from Eq. (26) for the above case, even for the time interval $t < 1$ s.

At larger times, when we can assume $\Gamma_2(t) \approx \Gamma_{20}$, the value of $\Delta\gamma_b$ tends to zero when it is proportional to $t^{-3/2}$, and further $\Delta\gamma$ values of the surfactant mixture become independent of the adsorption barrier and are described by Eq. (14), providing $c_{10} \gg c_{20}$ holds.

The comparison of experimental data with Eq. (14) is easier in the form

$$\left[\frac{d\gamma}{dt^{-1/2}}\right]_{t\to\infty} = \frac{RT\Gamma_{20}^2}{c_{20}}\sqrt{\frac{\pi}{4D_2}} \quad (35)$$

We recently showed [6] that adsorption barriers do not influence the time dependence of the surface tension $\gamma(t)$ at infinite time $t \to \infty$. The relation for a single non-ionic surfactant, known as the Hansen–Joos relation [18], is

$$\left[\frac{d\gamma}{dt^{-1/2}}\right]_{t\to\infty} = \frac{RT\Gamma_0^2}{c_0}\sqrt{\frac{\pi}{4D}} \quad (36)$$

while that of a 1:1 ionic surfactant takes the form [30]

$$\left[\frac{d\gamma}{dt^{-1/2}}\right]_{t\to\infty} = \frac{RT\Gamma_0^2}{c_0}\sqrt{\frac{\pi}{D}} \quad (37)$$

The time t used in Eqs. (35)–(37) is the effective adsorption times and can be calculated from Eq. (19).

3. Materials and methods

3.1. Dynamic surface tension measurements

The study of dynamic surface tension is performed using an automated maximum bubble pressure tensiometer (MTP-1 from Lauda). The principle and a detailed description of the method are given elsewhere [19,31]. It was shown earlier that the experimental results of this instrument agree very well with those obtained by other dynamic methods, such as the oscillating jet, the inclined plate and drop volume methods [17,31]. The standard version of the MPT-1 allows measurements in the time interval from 0.001 to 2 s. In the present paper, modified software was used which allowed measurements up to 50 s bubble time. The standard method works with a constant

gas flow at a given bubble frequency. Data at longer bubble times are obtained using a stopped flow regime. This was reached by switching off the gas flow through closing a magnetic valve, after a sufficiently low bubble frequency was reached. Owing to the further lowering of the surface tension with longer adsorption time (longer bubble time) the internal pressure in the system V_s, having a volume of about 50 cm^3, allows the production of further bubbles. The volume of each of the bubbles V_b is 2–5 mm^3, depending on the geometry of the measuring cell. The pressure inside the system P_s (approximately atmospheric pressure, 10^5 Pa) decreases with the detachment of one bubble by

$$\Delta P = P_s \frac{V_b}{V_s} \approx 4 - 10 \text{ Pa} \quad (38)$$

The detachment of each bubble corresponds to a surface tension decrease of

$$\delta\gamma = \Delta P r/2 \quad (39)$$

where r is the radius of the capillary (r = 0.0075 cm). The measured pressure in the system and the time interval between two bubbles leads to a time dependence of the surface tension at $t > 2$ s. The modified MPT-1 programme allows a fully automatic run of the standard procedure as well as of a stopped flow regime, leading to dynamic surface tensions in the respective time intervals. As an example, experimental results for two surfactant solutions are given in Fig. 1.

It has to be mentioned here that the stopped flow regime only works well at bubble times longer than 1.5 s, because of the slow pressure relaxation within the measuring cell of the MPT-1 (about 0.5 s). The potential of the stopped flow regime significantly increases the range of applications of the MTP-1. In particular, it can be used for the detection of traces of surface active contaminants in water.

3.2. Materials

Sodium alkyl sulphates (decyl, dodecyl and hexadecyl sulphate) were purified by extraction from hexane over 20 h with subsequent repeated recrystallisation from ethanol. The content of the admixtures did not exceed 1%. Chromatographic analysis of the purified specimens showed only lower homologues. Octylphenyl polyethylene glycol ethers $C_{14}H_{21}O(C_2H_4O)_nH$ (from Serva and Aldrich respectively) with different EO units (Triton X-45 (n = 4.5), Triton X-100 (n = 10), Triton X-114 (n = 11.4), Triton X-165 (n = 16.5), Triton X-305 (n = 30.5) and Triton X-405 (n = 40.5)) were used without further purification.

The aqueous surfactant solutions were prepared from a stock solution using doubly distilled and

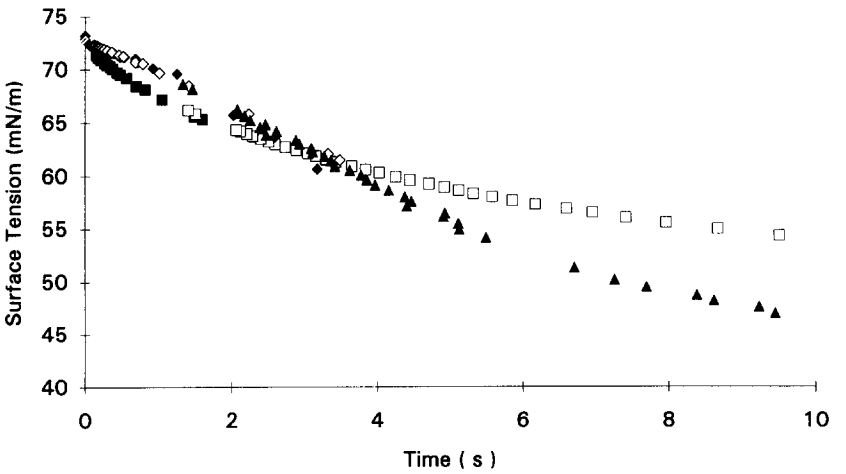

Fig. 1. Dynamic surface tension γ of Triton X-45 (◇, ◆, ▲) and X-100 (□, ■) at $c_0 = 0.05$ g l^{-1}; constant air flow regime (■, ◇, ◆); stopped flow regime (□, ▲).

deionised water. The last distillation was performed over alkaline $KMnO_4$ in a quartz still in order to remove traces of surface active impurities. The glass vessels, measuring cell and capillary used were cleaned with chromic acid, and rinsed carefully with distilled water.

4. Results and discussion

The experiments aim at the verification of Eq. (36) for single surfactant solutions and Eq. (35) for surfactant mixtures. We also tried to find the experimental conditions under which the time dependence of the surface tension shows irregularities owing to the desorption barriers, expected in mixed surfactant systems at a specific composition. In all the figures the dimension of the time axis is seconds.

The dynamic surface tension as a function of $1/\sqrt{t}$ of aqueous solutions of the six different non-ionics at 20°C is shown in Figs. 2–7. Over the range of longer adsorption times all the $\gamma(1/\sqrt{t})$-dependences are linear, as is expected from Eq. (36). The data of Triton X-100 at $c_0 = 1.55 \times 10^{-5}$ mol cm^{-3} (Fig. 6, curve 3) and Triton X-405 at $c_0 = 1.53 \times 10^{-5}$ mol cm^{-3} and $c_0 = 2.54 \times 10^{-5}$ mol cm^3 (Fig. 2, curves 1 and 2, respectively) agree very well with the data given in Ref. [32], which are obtained by another experimental technique.

The intersection of the linear parts of the curves in Figs. 2–7 with the ordinate give a good approximate of the equilibrium surface tension values $\gamma_\infty(c_0)$, from which the surface tension isotherms of the non-ionic surfactants can be constructed (Fig. 8). The calculation of the specific surfactant parameters Γ_∞ and b, as well as the equilibrium values of adsorption Γ_0 as functions of the bulk concentration c_0 from these isotherms, are performed on the basis of the following relations:

$$\Gamma_\infty = \frac{1}{RT}\left(\frac{d\gamma_\infty}{d \ln c_0}\right)_{c_0 \to CMC} \tag{40}$$

$$b = \left[\exp\left(\frac{\gamma_0 - \gamma_\infty}{RT\Gamma_\infty}\right) - 1\right] \Big/ c_0 \tag{41}$$

$$\Gamma_0 = \frac{bc_0}{1 + bc_0} \tag{42}$$

The results of calculations from Fig. 8 are summarised in Table 1, together with the values of $[d\gamma/d(1/\sqrt{t})]_{t \to \infty}$ determined from Figs. 2–7 and values of Γ_0 obtained from Eq. (36). The diffusion coefficients needed to calculate Γ_0 from Eq. (36) were interpolated/extrapolated from the values of Triton X-100 and Triton X-405 ($D_{X\text{-}100} =$

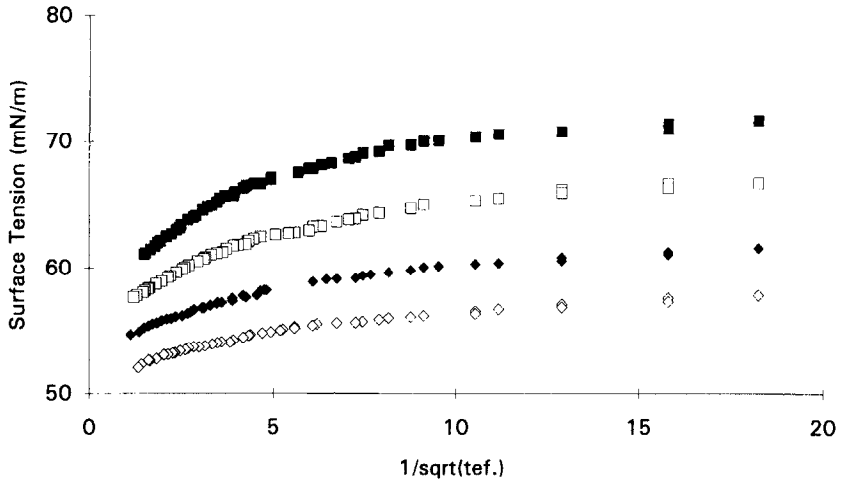

Fig. 2. Dynamic surface tension γ of Triton X-405 as a function of $(1/\sqrt{t})$ at different concentrations: $c_0 = 0.153$ (□), 0.254 (■), 0.508 (◆), 1.016 (◇) 10^{-6} mol cm^{-3}.

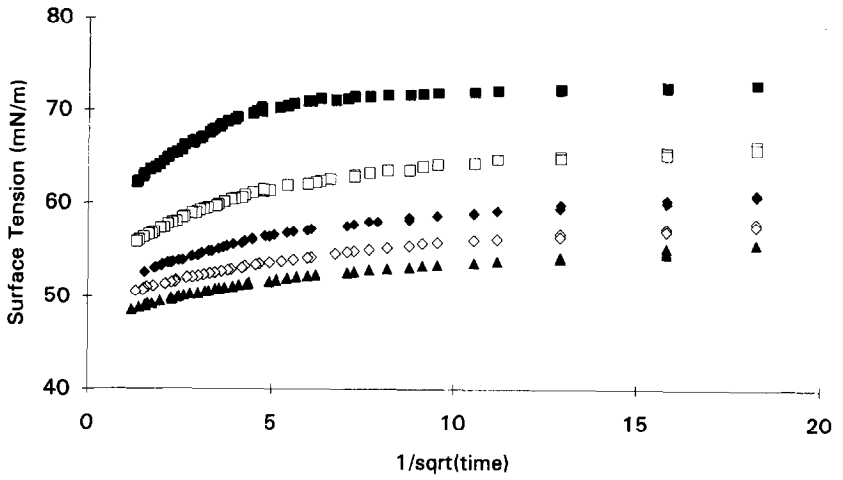

Fig. 3. Dynamic surface tension γ of Triton X-305 as a function of $(1/\sqrt{t})$ at different concentrations: $c_0 = 0.09$ (□), 0.226 (■), 0.452 (◆), 0.678 (◇), 0.903 (▲) 10^{-6} mol cm^{-3}.

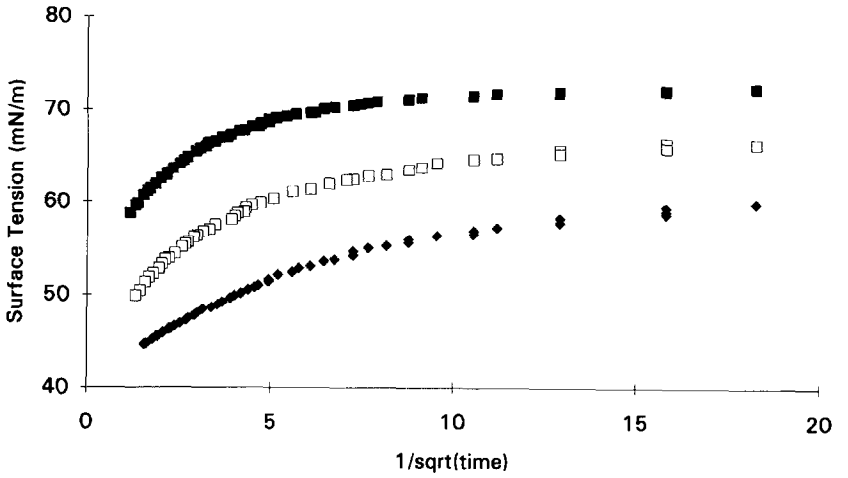

Fig. 4. Dynamic surface tension γ of Triton X-165 as a function of $(1/\sqrt{t})$ at different concentrations: $c_0 = 0.214$ (□), 0.536 (■), 1.072 (◆), 10^{-6} mol cm^{-3}.

8.8×10^{-7} cm^2 s^{-1}, $D_{X\text{-}405} = 7 \times 10^{-7}$ cm^2 s^{-1}) given in Refs. [32] and [33] using the molecular weights of the species and a correlation derived in Ref. [34].

From the data of Table 1 we can make the following conclusions:

— Eqs. (40)–(42) can be usefully applied to the Triton samples; the values of b do not vary significantly with concentration;

— the values of Γ_∞ decrease continuously with the number of EO units of the Tritons;

— the values of b do not change proportionally with the EO units of the Triton samples.

The most important result of the dynamic studies of the Triton samples is the good agreement between the equilibrium surface concentrations calculated from the adsorption isotherm and independently from Eq. (36). Thus we can conclude that the long time approximate solution (36) sufficiently describes the experimental data and that the studied Triton samples do not contain disturbing surface active impurities. Analogous

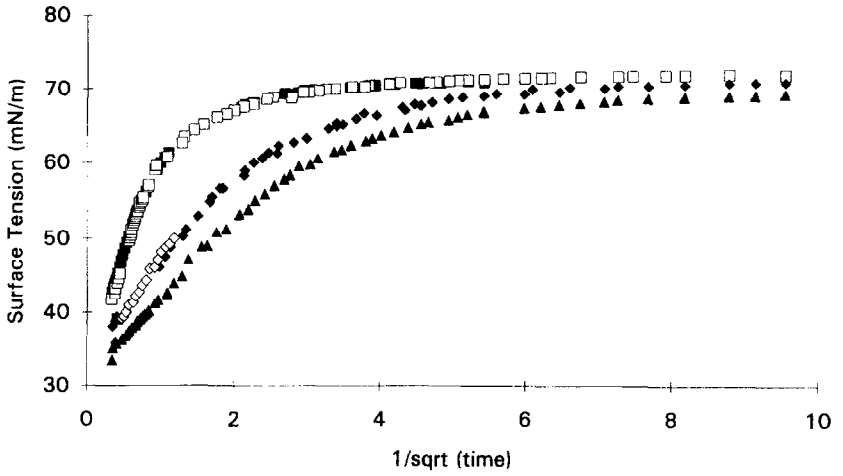

Fig. 5. Dynamic surface tension γ of Triton X-114 as a function of $(1/\sqrt{t})$ at different concentrations: $c_0 = 0.141$ (□, ■), 0.282 (◆, ◇), 0.423 (▲) 10^{-6} mol cm^{-3}.

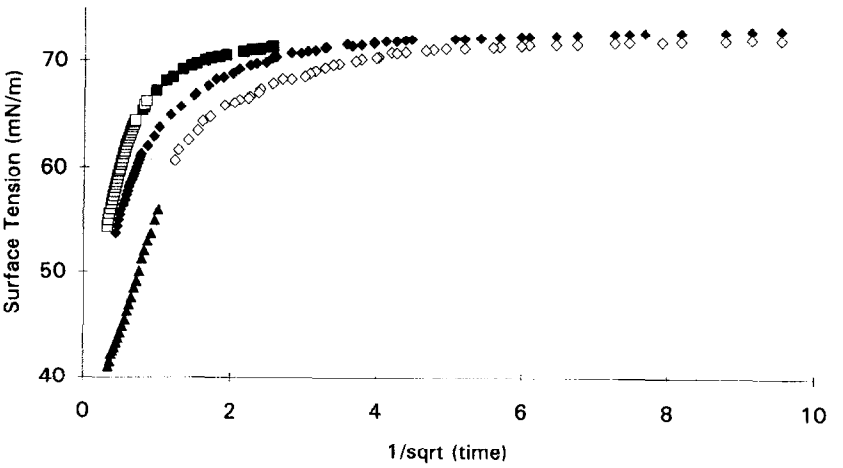

Fig. 6. Dynamic surface tension γ of Triton X-100 as a function of $(1/\sqrt{t})$ at different concentrations: $c_0 = 0.071$ (□, ■), 0.124 (◆), 0.155 (◇, ▲) 10^{-6} mol cm^{-3}.

conclusions were drawn earlier for the sodium alkyl sulphates used in the present study [6].

Fig. 9 shows the dynamic surface tensions obtained for mixtures of sodium hexadecyl sulphate (SHS) with sodium decyl (SDeS) and dodecyl sulphate (SDS), respectively. These data can be used to verify Eq. (35). From Eqs. (1), (2) and (42) we obtain

$$\Gamma_{20} = \bar{\Gamma}_{20}\frac{\Gamma_{2\infty}}{\Gamma_{\infty}}\left[1 + \frac{\bar{\Gamma}_{10}}{\Gamma_{2\infty}}\left(\frac{\Gamma_{2\infty} - \bar{\Gamma}_{20}}{\Gamma_{1\infty} - \bar{\Gamma}_{10}}\right)\right]^{-1} \quad (43)$$

where $\bar{\Gamma}_{10}$ and $\bar{\Gamma}_{20}$ are the surface concentrations of components 1 and 2, respectively, each at the same bulk concentration in the absence of the other. For the studied alkyl sulphates, the maximum adsorption is almost independent of alkyl chain length, $\Gamma_{1\infty} \approx \Gamma_{2\infty} \approx \Gamma_{\infty} = 3.5 \times 10^{-10}$ mol cm^{-2}. Values of Γ_{20} calculated from Eq. (43) and from the dynamic surface tension data in the form of $d\gamma/d(1/\sqrt{t})$ using Eq. (36) are summarised in Table 2. Good agreement between values from both sources has been reached.

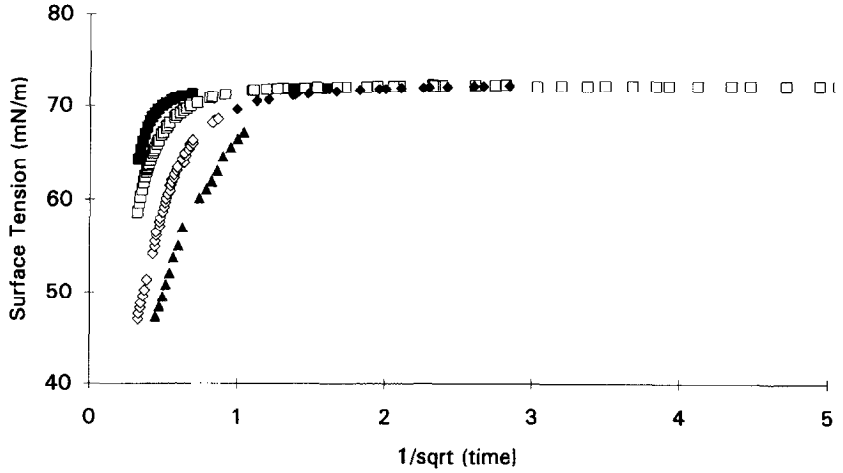

Fig. 7. Dynamic surface tension γ of Triton X-45 as a function of $(1/\sqrt{t})$ at different concentrations: $c_0 = 0.048$ (□), 0.071 (■), 0.118 (◇, ◆), 0.19 (▲) 10^{-6} mol cm^{-3}.

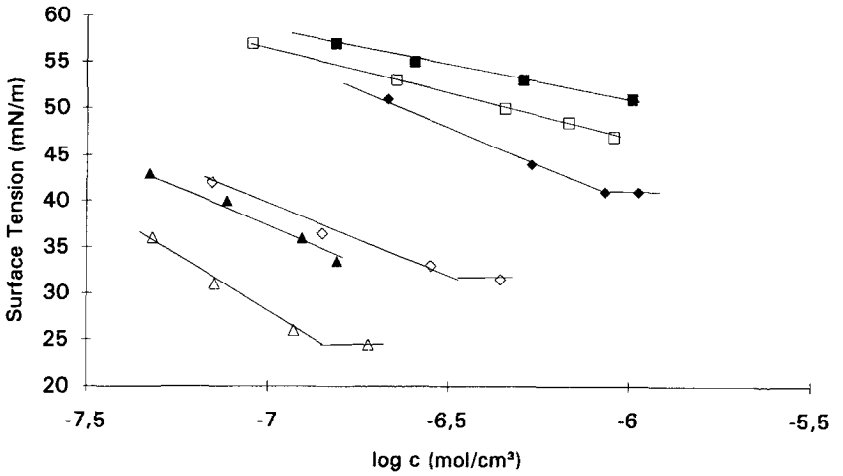

Fig. 8. Surface tension isotherms of different Triton samples at 20°C; X-405 (□), X-305 (■), X-165 (◆), X-114 (◇), X-100 (▲), X-45 (△).

Some results of the dynamic surface tensions of mixtures of SDeS and SDS with Triton surfactants are shown in Figs. 10–12. At small adsorption times t, only the alkyl sulphate component adsorbs. At $1/\sqrt{t} < 10\ \mathrm{s}^{-1/2}$ the values of γ become significantly lower than the values of the corresponding solutions containing only alkyl sulphate. In this exact time interval, the Triton species start to adsorb effectively, which becomes clear from the data given in Figs. 4–7. There are a number of pecularities in the paths of some of the curves in Figs. 10–12, which will be discussed later.

Some results from mixtures of Triton X-405 with Triton samples of lower molecular weight are shown in Fig. 13. Compared with the data in Figs. 4–7, it becomes evident that at small t only the Triton X-405 adsorbs, the higher surface active Tritons starting adsorbing at larger times. The

Table 1
Adsorption parameters of Triton samples at the water–air interfaces at 20°C

Substance Γ_∞ (mol cm^{-2}) D (cm^2 s^{-1})	c_0 (mol m^{-3})	γ_∞ (mN m^{-1})	b (m^3 mol^{-1})	$\left(\frac{d\gamma}{d(1/\sqrt{t})}\right)_{t\to\infty}$ ($s^{1/2}$ mN m^{-1})	Γ_0 (Eq. 42) (10^{-10} mol cm^{-2})	Γ_0 (Eq. 36) (10^{-10} mol cm^{-2})
X-405	0.153	57	716	2.2	1.4	1.3
1.4×10^{-10}	0.254	55	780	1.7	1.4	1.3
7×10^{-7}	0.508	53	704	1.0	1.4	1.4
	1.016	51	655	0.6	1.4	1.5
X-305	0.090	57	410	3.2	1.8	1.1
1.8×10^{-10}	0.226	53	412	2.0	1.8	1.3
7.3×10^{-7}	0.452	50	410	1.3	1.8	1.5
	0.678	48.5	385	1.0	1.8	1.6
	0.903	47	407	1.0	1.8	1.9
X-165	0.214	51	114	4.4	2.7	2.0
2.8×10^{-10}	0.536	44	131	4.0	2.8	3.0
7.3×10^{-7}	0.857	41	128	2.0	2.8	2.7
X-114	0.070	42	853	28	3.0	2.9
3.1×10^{-10}	0.141	36.5	828	22	3.1	3.7
8.6×10^{-7}	0.282	33	705	14	3.1	4.1
X-100	0.047	43	871	46	3.2	3.1
3.3×10^{-10}	0.077	40	778	38	3.2	3.6
8.8×10^{-7}	0.124	36	800	30	3.3	4.0
	0.155	33.5	823	22	3.3	3.9
X-45	0.048	36	433	90	4.6	4.5
4.8×10^{-10}	0.071	31	496	80	4.7	5.1
9.5×10^{-7}	0.118	26	424	62	4.8	5.9

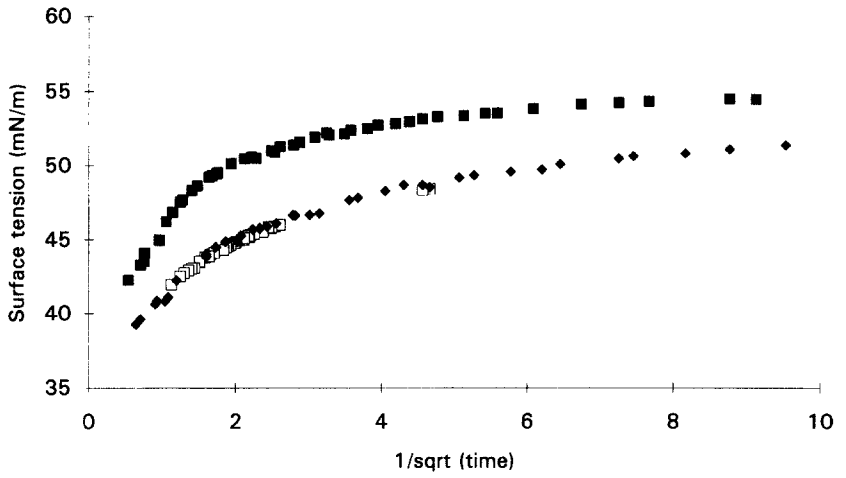

Fig. 9. Dynamic surface tension of alkyl sulphate mixtures at 40°C; 2×10^{-6} mol cm^{-3} SDeS + 0.5×10^{-6} mol cm^{-3} SHS (□), 5×10^{-6} mol cm^{-3} SDS + 0.5×10^{-6} mol cm^{-3} SHS (■, ◆).

Table 2
Adsorption characteristic of mixtures of sodium alkylsulphate at 40°C

Components of mixtures	c_{i0} (mol m^{-3})	$\bar{\Gamma}_{i0}$ (10^{-10} mol cm^{-2})	D_2 (10^{-6} cm^2 s^{-1})	$\left(\frac{d\gamma}{dt^{-1/2}}\right)_{t\to\infty}$ (mN m^{-1} s$^{1/2}$)	Γ_{20} (10^{-10} mol cm^{-2})	
					Eq. (43)	Eq. (35)
(1) SDeS +	12	2.0				
(2) SHS	0.5	3.2	2.3	6.0	2.9	3.4
(1) SDS +	5.0	2.8				
(2) SHS	0.5	3.2	2.3	4.0	2.4	2.7

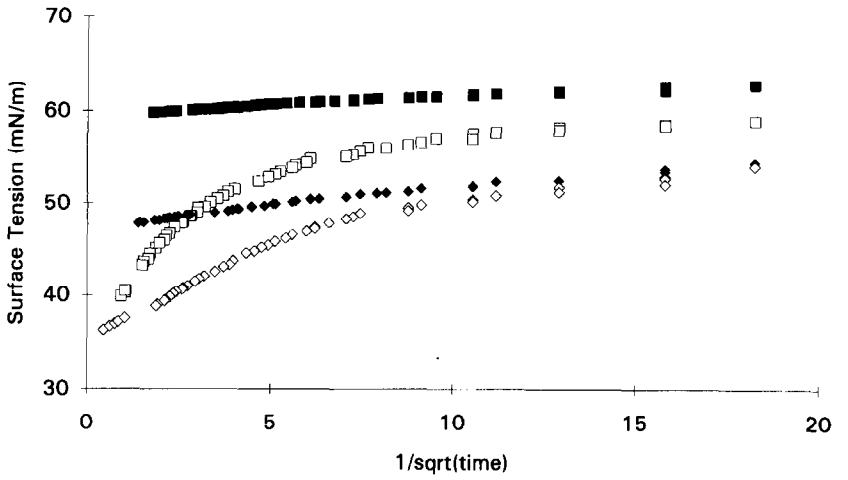

Fig. 10. Dynamic surface tension γ as a function of $(1/\sqrt{t})$ of mixed surfactant solutions; 10^{-5} mol cm^{-3} SDeS without (□) and mixed with (■) 2.82×10^{-7} mol cm^{-3} Triton X-114, 5×10^{-6} mol cm^{-3} SDS without (◆) and mixed with (◇) 0.282×10^{-6} mol cm^{-3} Triton X-114.

results of calculations of the adsorption of Triton species added to SDeS, SDS and Triton X-405 on the basis of Eq. (35) are summarised in Table 3. The data show the following general trend: in all cases $\Gamma_{20} < \bar{\Gamma}_{20}$ and Γ_{20} increases at the same bulk concentration according to the sequence SDS, SDeS, Triton X-405, i.e. with decreasing surface activity of component 1. Accurate calculation of Γ_{20} from Eq. (43) is complicated for these systems, owing to the differences in the $\Gamma_{i\infty}$-values for the mixture components. Correct calculation would be possible using a Frumkin–Damaskin isotherm as mentioned above [13,14]. An approximate calculation for the present systems is possible using an equation derived by Lucassen–Reynders [35,36]:

$$\ln(\Gamma_{20}/\Gamma_{10}) = \ln(\bar{\Gamma}_{20}/\bar{\Gamma}_{10}) + \frac{\Pi_2}{RT\Gamma_{2\infty}} - \frac{\Pi_1}{RT\Gamma_{1\infty}} + \frac{\Pi}{RT}\left(\frac{1}{\Gamma_{1\infty}} - \frac{1}{\Gamma_{2\infty}}\right) \quad (44)$$

where Π_1 and Π_2 are the surface pressures of the solutions of the individual components only, while Π is the value for the mixture. The results obtained from Eq. (44) are in qualitative agreement with those calculated from the dynamic surface tensions and given in Table 3.

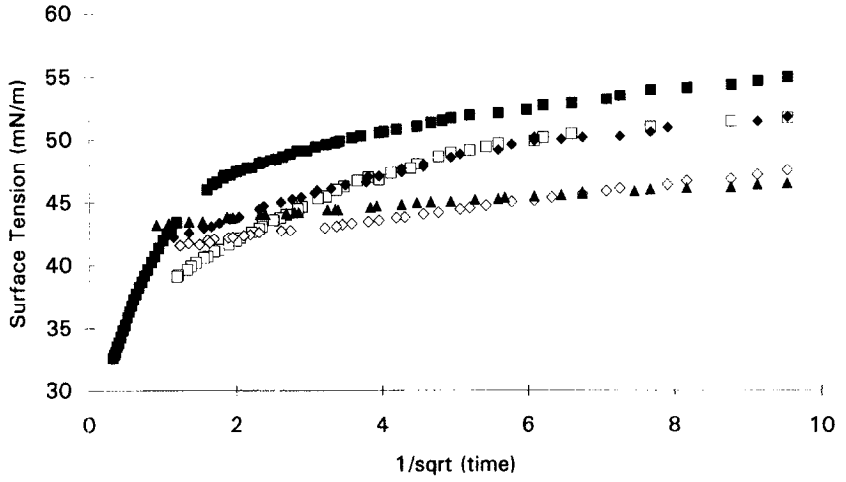

Fig. 11. Dynamic surface tension γ as a function of $(1/\sqrt{t})$ of 5×10^{-6} mol cm^{-3} SDS mixed with 0.118×10^{-6} mol cm^{-3} Triton X-45 (□), 0.155×10^{-6} mol cm^{-3} Triton X-100 (■), 0.214×10^{-6} mol cm^{-3} Triton X-165 (◆), 0.536×10^{-6} mol cm^{-3} Triton X-165 (◇), and 0.452×10^{-6} mol cm^{-3} Triton X-305 (▲).

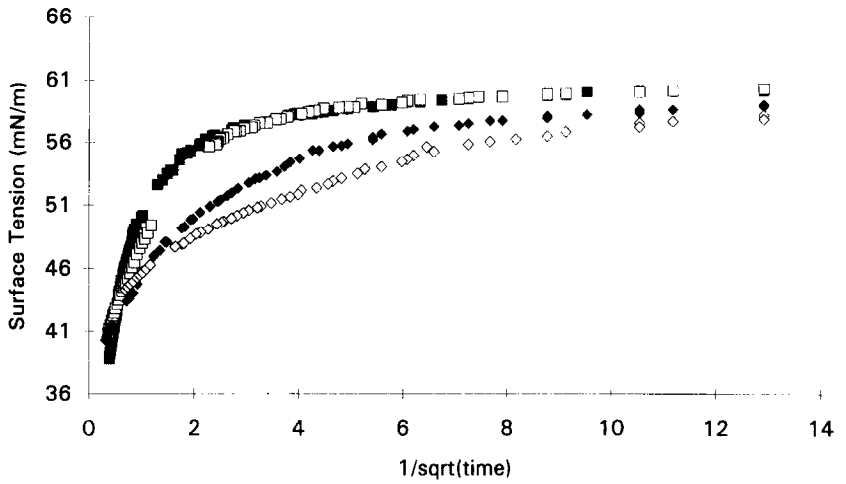

Fig. 12. Dynamic surface tension γ as a function of $(1/\sqrt{t})$ of 10^{-5} mol cm^{-3} SDeS mixed with 0.118×10^{-6} mol cm^{-3} Triton X-45 (□), 0.077×10^{-6} mol cm^{-3} Triton X-100 (■), 0.155×10^{-6} mol cm^{-3} Triton X-100 (◆), and 0.282×10^{-6} mol cm^{-3} Triton X-114 (◇).

Let us return to an analysis of the pecularities in the dynamic surface tensions located over a time interval in which the second component starts to adsorb, leading to desorption of the main component. This desorption is indicated by a significant further decrease in surface tension and a change in the slope of the $\gamma(1/\sqrt{t})$-dependence compared to the single main component.

The time interval of the onset of desorption of the main component is shown in Fig. 14 for the mixtures of SDeS and SDS with Triton X-114 and X-165 on a magnified scale. At $t \approx 0.02$ s, the dynamic surface tensions exhibit a small transition zone of constant surface tension values corresponding to a jump in the order of 0.4 mN m^{-1}, which is in the order of magnitude of the absolute accuracy of the instrument used. As the relative accuracy of the instrument MPT-1 is two to three times

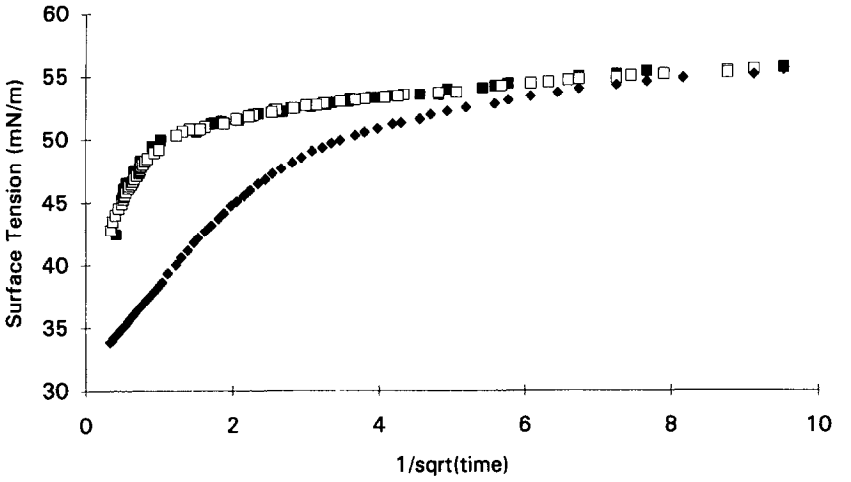

Fig. 13. Dynamic surface tension γ as a function of $(1/\sqrt{t})$ of 1.016×10^{-6} mol cm^{-3} Triton X-405 mixed with 0.118×10^{-6} mol cm^{-3} Triton X-45 (□), 0.077×10^{-6} mol cm^{-3} Triton X-100 (■), and 0.282×10^{-6} mol cm^{-3} Triton X-114 (◆).

Table 3
Adsorption characteristic of surfactant mixtures at 20°C

Added compound c_2^0 (mol m^{-3})	Basic surfactant[a]	$\bar{\Gamma}_{20}$ (10^{-10} mol cm^{-2})		$\left(\frac{d\gamma}{dt^{-1/2}}\right)_{t\to\infty}$ (mN m^{-1} s$^{1/2}$)	Γ_{20} (10^{-10} mol cm^{-2})
		From isotherm	From $\gamma(t)$		
Triton X-45	1	4.7	5.9	16	2.9
0.188	2			21	3.3
	3			32	4.1
Triton X-100	1	3.2	3.5	7	1.5
0.077	2			12	2.0
	3			17	2.4
0.155	1	3.3	3.9	3.2	1.5
	2			6.5	2.0
	3			7	2.1
Triton X-114	1	3.1	4.1	2.0	1.6
0.282	2			5.7	2.6
	3			6.8	2.9
Triton X-165	1	2.7	2.0	2.0	1.4
0.214	2			4.0	2.2
	3			6.5	2.8
0.536	1	2.8	3.0	0.8	1.4
Triton X-305	1	1.8	1.3	0.4	0.8
0.452					

[a] 1: SDS; $c_{10} = 5 \times 10^{-6}$ mol cm^{-3}, $\bar{\Gamma}_{10} = 3 \times 10^{-10}$ mol cm^{-2}. 2: SDeS; $c_{10} = 10^{-5}$ mol cm^{-3}, $\bar{\Gamma}_{10} = 2 \times 10^{-10}$ mol cm^{-2}. 3: Triton X-405; $c_{10} = 1.016 \times 10^{-6}$ mol cm^{-3}, $\bar{\Gamma}_{10} = 1.4 \times 10^{-10}$ mol cm^{-2}.

better and almost all measurements are reproduced by a second run, these effects seem to be real.

On addition of Triton X-45 or X-100 to SDS or SDeS solutions, the surface tension jumps appear at a time of about 0.1 s and amount to less than 0.2 mN m^{-1}; therefore, they are not significant

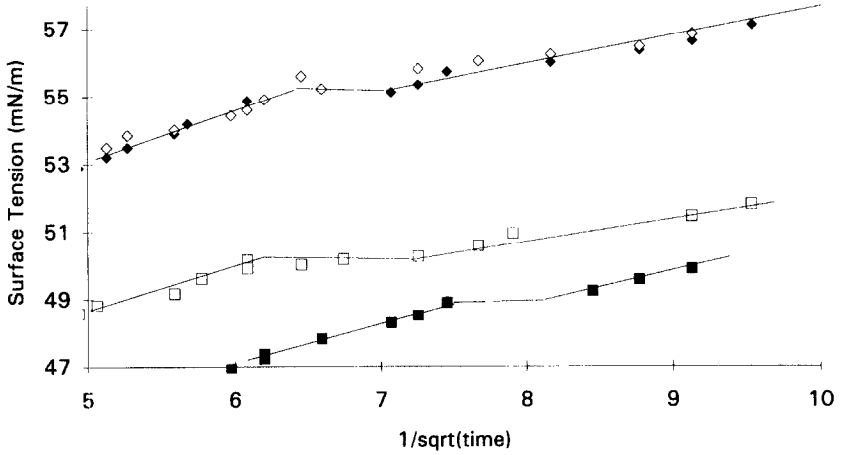

Fig. 14. Range of displacement of one component of a surfactant mixture at the interface studied by dynamic surface tension γ as a function of $(1/\sqrt{t})$: 5×10^{-6} mol cm^{-3} SDS + 0.282×10^{-6} mol cm^{-3} Triton X-114 (□); 5×10^{-6} mol cm^{-3} SDS + 0.214×10^{-6} mol cm^{-3} Triton X-165 (■); 10^{-5} mol cm^{-3} SDeS + 0.282×10^{-6} mol cm^{-3} Triton X-114 (◆); 10^{-5} mol cm^{-3} SDeS + 0.214×10^{-6} mol cm^{-3} Triton X-165 (◇).

under the present experimental conditions. If we change to Triton X-405 as the main surfactant and use Triton X-45 or X-100 as the second component, a surface tension jump of the order of 0.4 mN m^{-1} is again observed (Fig. 15). Addition of other Tritons of higher molecular weight, such as X-305, show the same result as observed with SDS and SDeS, and any irregularities measured are within the accuracy of the instrument.

If we assume that the observed jumps in Figs. 14 and 15 are real, we can interpret the data on the basis of Eq. (26) in terms of the rate constant of desorption k_{des}. Results of these estimations are summarised in Table 4, for which the values of Γ_{20} are taken from Table 3 and the values of $\Gamma_2(t)$ are calculated from Eq. (17). The time t^* defines the moment at which the surface tension jump occurs. The values of the rate constant k_{des} of SDS and

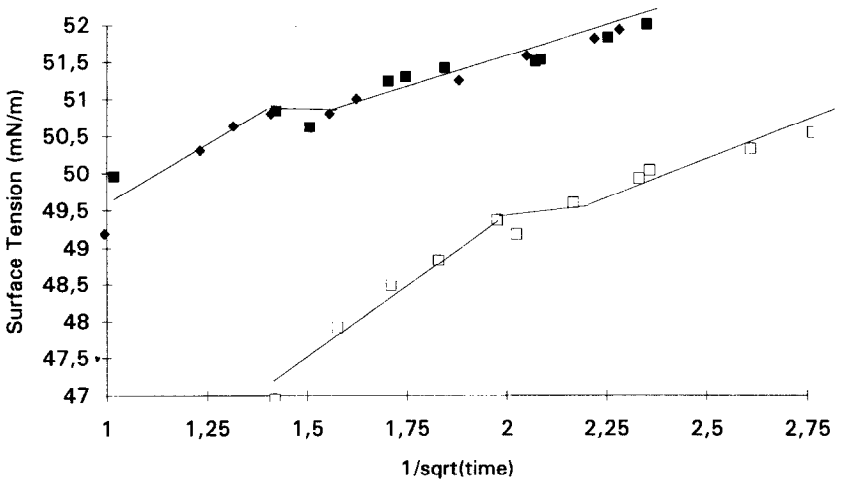

Fig. 15. Range of displacement of 1.016×10^{-6} mol cm^{-3} Triton X-405 by a second surfactant at the interface studied by dynamic surface tension γ as a function of $(1/\sqrt{t})$: 0.115×10^{-6} mol cm^{-3} Triton X-45 (□); 0.236×10^{-6} mol cm^{-3} Triton X-45 (■); 0.077×10^{-6} mol cm^{-3} Triton X-100 (◆).

Table 4
Calculated rate constants of adsorption of the main component from the plateau region in the dynamic surface tension dependence

Mixture (concentration in mol m^{-3})	Γ_{20} (10^{-10} mol cm^{-2})	Γ_2 (10^{-10} mol cm^{-2})	t^* (s)	$\Delta\gamma_b$ (mN m^{-1})	k_{ad} (s^{-1})
(1) Triton X-405 (1.016) + (2) Triton X-45 (0.118)	4.1	0.72	0.4	0.3	6
(1) Triton X-405 (1.016) + (2) Triton X-100 (0.077)	2.4	0.44	0.4	0.3	4
(1) SDS (5.0) + (2) Triton X-165 (0.214)	1.4	0.27	0.025	0.3	35
(1) SDS (5.0) + (2) Triton X-114 (0.282)	1.6	0.30	0.016	0.4	52
(1) SDeS (10.0) + (2) Triton X-165 (0.214)	2.2	0.29	0.025	0.3	41
(1) SDeS (10.0) + (2) Triton X-114 (0.282)	2.6	0.39	0.025	0.4	40

SDeS amount to about 40 s^{-1} and agree well with those obtained by Bleys and Joos [22], who found $k_{des} \approx 80\ s^{-1}$. The rate constant of Triton X-405 is $k_{des} \approx 5\ s^{-1}$, which is about one order of magnitude smaller. This may be caused by a much slower process of reorientation of the hydrophilic oxyethylene chains (40 EO groups in the Triton X-405 molecules) which are assumed to be located at the surface.

Eq. (26) represents the contribution of a barrier controlled contribution to the dynamic surface tension $\Delta\gamma_b$, and is a monotonic function with a maximum at $t = 0$, tending to zero at large t. The reason for a temporarily constant surface tension γ at $t = t^*$ is, in our opinion, due to a hindered desorption of the main component at times smaller than the time corresponding to the desorption rate $t = 1/k_{des}$. If we use t_2 to denote the time needed by a second component of higher surface activity in a mixture to adsorb significantly, we can formulate the conditions under which the observed peculiarities may appear. For $1 \ll t_2 k_{des}$ no temporary plateau in the $\gamma(t)$-curves is expected, while for $1 \gg t_2 k_{des}$ such a plateau may occur.

Another explanation of the plateau region or a surface tension jump in a $\gamma(t)$-curve can also be given on the basis of a pure diffusion controlled model of a surfactant mixture, assuming a significantly smaller maximum surface concentration $\Gamma_{\infty 1}$ compared with that of the second component $\Gamma_{\infty 2}$. This conclusion follows directly from Eqs. (9), (10), (14) and (16) under the condition $\Gamma_{\infty 1} \leqslant 2\Gamma_{\infty 2}$.

Possible dynamic surface tension behaviour of surfactant mixtures is schematically shown in Fig. 16. The appearance of a transition region II corresponds to a mixture of a fast adsorbing surfactant occupying a large surface area and a slowly adsorbing compound demanding only a small area at the interface. The transition region is located in the time interval of desorption of the first component owing to competitive adsorption of the second one. Such a situation exists for the system SDS + dodecanol, a typical system studied, for example, in Ref. [7], where exactly this type of $\gamma(t)$-curve was observed. If an additional significant area dilation is overlapped by the adsorption/desorption process, such as in the growing drop experiment published by MacLeod and Radke [10], even a minimum in the $\gamma(t)$-dependence can be observed. This case is demonstrated by the transition curve I as a dotted line in Fig. 16.

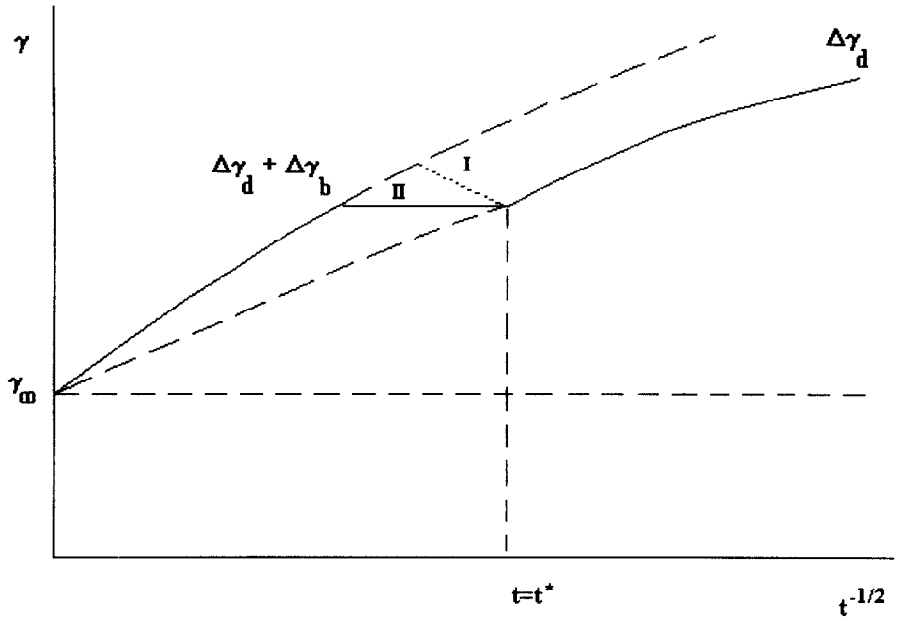

Fig. 16. Schematic of the surface tension change according to a pure diffusion controlled ($\Delta\gamma_d$) and mixed adsorption model ($\Delta\gamma_d + \Delta\gamma_b$); $t = t^*$ corresponds to the time at which desorption of the main component sets in due to competitive adsorption of a second component; transition I is caused by a desorption barrier overlapped by an additional surface area increase, and transition II is caused by a desorption barrier only.

5. Conclusions

The Hansen–Joos theory was generalised for surfactant mixtures including the case of non-diffusion controlled adsorption. In the case where desorption of the main surfactant starts after a second higher surface active surfactant begins to adsorb, a relation is derived also taking into consideration a barrier controlled process of the main component.

Adsorption of the individual surfactants used in the present study is diffusion controlled. In some mixtures temporary plateaus in the $\gamma(t)$-curves are observed, which are interpreted well by a definite desorption rate constant k_{des}; this is in good agreement with values determined by other authors.

The maximum bubble pressure tensiometer MPT-1 was modified to also allow measurements at higher adsorption times up to 100 s; this was achieved by simply changing the software that came with the instrument.

Acknowledgements

We thank S.V. Lylyk for the excellent performance of the experiments. We are very grateful to Professor Paul Joos for a very helpful discussion. The work was financially supported by projects of the European Community (HCM ERBCHRXT-930322 and INTAS 93-2463), the DFG (Wu187/3-1) and the Senate of Berlin (ERP 2659).

References

[1] R. Miller and G. Kretzschmar, Adv. Colloid Interface Sci., 37 (1991) 97.
[2] P. Van den Bogaert and P. Joos, J. Phys. Chem., 84 (1980) 190.
[3] R. Miller and K. Lunkenheimer, Colloid Polym. Sci., 260 (1982) 1148.
[4] V.B. Fainerman, Ju.M. Rakita, S.V. Lylyk and V.M. Zadara, Zh. Fiz. Khim., 61 (1987) 131.
[5] J.P. Fang and P. Joos, Colloids Surfaces, 65 (1992) 113.

[6] V.B. Fainerman, A.V. Makievski, and R. Miller, Colloids Surfaces A: Eng. Aspects, 87 (1994) 61.
[7] G. Czichocki, D. Vollhardt and H. Seibt, Tenside Detergents, 18 (1981) 320.
[8] D. Vollhardt and G. Czichocki, Langmuir, 6 (1990) 317.
[9] K. Lunkenheimer and G. Czichocki, J. Colloid Interface Sci., 160 (1993) 509.
[10] C.A. MacLeod and C.J. Radke, J. Colloid Interface Sci., 160 (1993) 435.
[11] A. Bonfillon and D. Langevin, Langmuir, 9 (1993) 2172.
[12] V.B. Fainerman, Colloids Surfaces, 57 (1991) 249.
[13] B.B. Damaskin, Elektrochimija, 5 (1969) 356.
B.B. Damaskin, A.N. Frumkin and N.A. Borovaja, Elektrokhimija, 6 (1972) 807.
[14] R. Wüstneck, R. Miller and J. Kriwanek, Colloids Surfaces, 81 (1993) 1.
[15] A.F. Ward and L. Trodai, J. Phys. Chem., 14 (1946) 453.
[16] R. Miller, K. Lunkenheimer and G. Kretzchmar, Colloid Polym. Sci., 257 (1979) 1118.
[17] R. Miller, P. Joos and V.B. Fainerman, Adv. Colloid Interface Sci., 49 (1994) 249.
[18] P. Van den Bogaert and P. Joos, J. Phys. Chem., 83 (1979) 2244.
[19] V.B. Fainerman, Colloids Surfaces, 62 (1992) 333.
[20] R. Miller, Colloid Polym. Sci., 258 (1980) 179.
[21] P. Joos and E. Rillaerts, J. Colloid Interface Sci., 79 (1981) 96.
[22] G. Bleys and P. Joos, J. Phys. Chem., 89 (1985) 1027.
[23] F. Van Voorst Vader, Th.F. Erkelens and M. van den Tempel, Trans. Faraday Soc., 60 (1964) 1170.
[24] E. Rillaerts, and P. Joos, J. Phys. Chem., 86 (1982) 3471.
[25] J.F. Baret, J. Chim. Phys., 65 (1968) 895.
[26] J.T. Davies and E.K. Rideal, Interfacial Phenomena, Academic Press, New York, 1963.
[27] F.T. Lindström, R. Haque and W.R. Coshow, J. Phys. Chem., 74 (1970) 495.
[28] V.B. Fainerman, Koll. Zh., 36 (1974) 1112.
[29] V.B. Fainerman, Uspechi Khim., 54 (1985) 1613.
[30] G. Serrien and P. Joos, J. Colloid Interface Sci., 139 (1990) 149.
[31] V.B. Fainerman, R. Miller and P. Joos, Colloid Polym. Sci., 272 (1994) 731.
[32] J. Van Hunsel and P. Joos, Colloids Surfaces, 24 (1987) 139.
[33] R.M. Weinheimer, D.F. Evans and E.L. Cussler, J. Colloid Interface Sci., 80 (1981) 357.
[34] R. Reid, J. Prausnistz and Th. Sherwood, The Properties of Gases and Liquids, McGraw-Hill, New York, 1977.
[35] E.H. Lucassen-Reynders, J. Colloid Interface Sci., 41 (1972) 156.
[36] E.H. Lucassen-Reynders, J. Colloid Interface Sci., 85 (1982) 178.